INTERNATIONAL JOURNAL OF PRECISION ENGINEERING AND MANUFACTURING Vol. 17, No. 3, pp. 323-329 MARCH 2016 / 323
DOI: 10.1007/s12541-016-0040-x ISSN 2234-7593 (Print) / ISSN 2005-4602 (Online)

Position-based Impedance Control for Force Tracking of a Wall-Cleaning Unit

Taegyun Kim[1], Hwa Soo Kim[2,#], and Jongwon Kim[1]

1 School of Mechanical and Aerospace Engineering, Seoul National University, 1 Gwanak-ro, Gwanak-gu, Seoul, 08826, South Korea
2 Department of Mechanical System Engineering, Kyonggi University, 154-42, Gwanggyosan-ro, Yeongtong-gu, Suwon-si, Gyeonggi-do, 16227, South Korea
Corresponding Author / E-mail: hskim94@kgu.ac.kr, TEL: +82-31-249-9806, FAX: +82-31-244-6300

KEYWORDS: Impedance control, Force tracking, Stiffness adaptation, Wall cleaning

This paper presents a position-based impedance control scheme for force tracking of a wall-cleaning unit installed on the wall-climbing mobile platform ROPE RIDE. It is important to maintain a contact force between the wall-cleaning unit and various types of walls in order to guarantee good cleaning performance. For this purpose, the target stiffness of impedance model as well as the reference position command for the wall-cleaning unit are tactfully adjusted according to the force tracing error between the real and reference contact forces. In comparison with existing impedance control methods, the proposed impedance control scheme is not only simple to implement but also robust against external disturbances such as varying trajectory or stiffness of walls as well as model uncertainties of cleaning unit. As a result, the proposed impedance control scheme can promise acceptable force tracking error in the steady state even for various trajectories of wall and varying reference forces. The stability and performance of proposed impedance control scheme are theoretically examined and the extensive experiments using the wall-cleaning unit are carried out to prove the force tracking capability of the proposed impedance control scheme.

Manuscript received: January 20, 2015 / Revised: August 26, 2015 / Accepted: September 23, 2015

NOMENCLATURE

M, B, K = target mass, damping and stiffness parameters for the impedance control
k_0, k_e = modified target stiffness and wall stiffness
x_d, x_c = desired and compliant trajectories of manipulator
x_d^0 = initial condition for desired trajectory
x_{dc} = trajectory correction defined by $x_{dc} = x_d - x_c$
x_e, x = wall trajectory and real trajectory of end-effector
δx = position tracking error between compliant and real trajectories
$\bar{x}_e$ = wall trajectory combined with position tracking error
F, F_{ref} = real contact force and reference force
E_f = force tracking error between real contact force and reference force
k_p, k_d, k_i = proportional, derivative and integral control gains
η = positive control gain for desired trajectory correction
$X_e(s)$, $E_f(s)$, $X_d^0(s)$, $F_{ref}(s)$ = Laplace transforms of $\bar{x}_e$, E_f, x_d^0 and F_{ref}
$\Delta(s)$ = characteristic equation of transfer function from $X_e(s)$ to $E_f(s)$

1. Introduction

Over the last decade, the robot manipulators have been widely adopted to perform a variety of industrial tasks like manufacturing, maintenance and inspection operations so that they have the chance of interacting with an environment or an object frequently. Therefore, a suitable control strategy is indispensable for regulating a contact force between the manipulator and the environment.[1-8]

From this viewpoint, it is not surprising that many investigations have been made to solve this challenge and among existing schemes to control the interaction between the manipulators and environments, the impedance control is well known for its simplicity and acceptable performance, which controls the robot manipulator to interact with the environment compliantly by establishing a virtual mass-spring-damper system.[3] However, the force tracking ability cannot be ensured via the impedance control and furthermore, unknown stiffness and trajectory of environment as well as the inaccurate model of robot manipulator make it worse to achieve the desired force tracking performance.

To enhance the force tracking performance of impedance control scheme against those uncertainties, Seraji et al. modified the reference trajectory of manipulator on the basis of the estimation of stiffness and

position of environment but in practical applications, it is difficult to obtain exact values of stiffness and position of environment in real time.[9-11] Jung et al. proposed the adaptation of impedance model with zero-stiffness and its tracking performances for a constant reference force were verified through experiments using the industrial robot.[12] However, when the dynamic model of manipulator drastically changes, for examples, its main platform climbs up an obstacle, its performance may be deteriorated. In the similar manner, Lee et al. suggested the adaptation of target stiffness of impedance model according to the force tracking error but this method can guarantee its zero force tracking capability in the steady state only for the zero reference force and the stiffness of environment should be known for its stability.[13]

In this paper, a new position-based impedance control scheme is presented for force tracking of the wall-cleaning unit. The dynamic relation between the tracking error and the varying trajectory of the manipulator as well as the varying reference force is derived in details and the stability of proposed control scheme is exhaustively analyzed without information on the trajectory or stiffness of environment. The stability analysis verifies that the proposed impedance control scheme can guarantee the zero steady state force tracking error even for varying trajectories and unknown stiffness of environment. The extensive experiments using the wall-cleaning unit for the wall-climbing mobile platform are performed under varying trajectories of environment.

The rest of this paper is organized as follows. Section II introduces the wall-cleaning unit for the wall-climbing mobile platform ROPE RIDE. In Section III, The proposed impedance control scheme is described and its stability as well as tracking performance are analyzed. Under varying trajectories of environment, the experiments using the wall-cleaning unit are carried out to prove the tracking capability of proposed impedance control scheme in Section IV.

2. Wall-climbing Mobile Robotic Platform

2.1 Introduction of wall-climbing mobile robotic platform (ROPE RIDE)

The wall-climbing mobile platform called as ROPE RIDE was designed to perform various operations on high-rise buildings instead of a human and one of its main functions is to climb up various types of walls efficiently.[14] As shown in Fig. 1, the ROPE RIDE is composed of two main bodies: the upper and lower bodies connected by a passive R-joint. While the rope ascender, the payload interface and the steering mechanism are installed in the upper body of ROPE RIDE, two propeller thrusters and four triangular tracks are installed in its lower body, respectively. The payload such as a cleaning unit is installed in the upper body of ROPE RIDE by using the payload interface.

Note that the passive R-joint is adopted not only to prevent the unexpected moments acting on the lower body directly but also to lower the center of mass of ROPE RIDE so that such instability as tip-over is prevented. Also, since the ROPE RIDE on high-rise building is probably exposed to strong winds, its moving trajectory may be deviated from the desired one. In order to cope with such deviation and also increase the workspace of ROPE RIDE, the steering mechanism is used, which enables the ROPE RIDE to rotate from -90° to 90°.

Four triangular tracks are used for smooth obstacle-overcoming

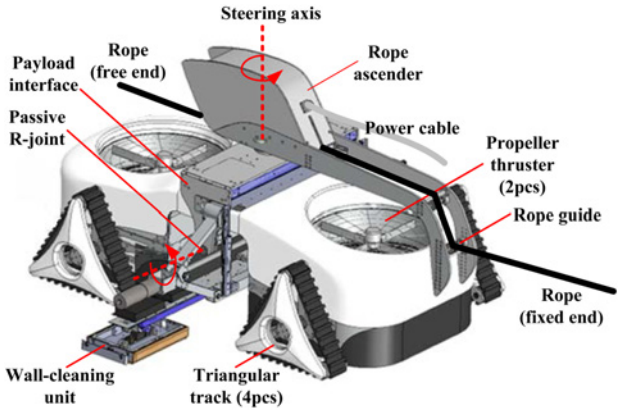

Fig. 1 Kinematic structure of wall-climbing mobile platform ROPE RIDE

Table 1 Specifications of ROPE RIDE

Items	Specification
Size	957(L) × 1500(W) × 758(H) mm^3
Weight	75 kg
Climbing speed	15 m/min
Payload	20 kg
Power	External cable
User interface	Wireless control + wireless camera
Climbing method	Rope ascender + triangular track

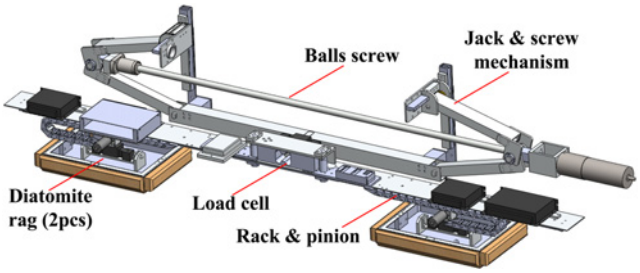

Fig. 2 1-DOF wall-cleaning unit for ROPE RIDE

without complicated control technique or recognition of obstacle. Two propeller thrusters are adopted to ensure good contact with a wall. Table 1 summarizes the specifications of ROPE RIDE and for more details of ROPE RIDE, refer to the reference.[14]

2.2 Wall-cleaning unit for ROPE RIDE

A 1-DOF wall-cleaning unit installed on the ROPE RIDE was designed to carry out a wall-cleaning task as shown in Fig. 2, where a jack & screw mechanism is used to push two diatomite rags towards a wall during wall-cleaning. Without using water, two diatomite rags remove the dust from a wall while moving from side to side along a rack & pinion. Four switch-type contact detection sensors are installed in the front/lateral sides of each cleaning rag. A load cell is installed in the center of cleaning unit to measure the actual contact force between the cleaning unit and a wall.

It is worthwhile to note that in order to guarantee the acceptable

cleaning performance, the contact force between the cleaning unit and the wall should be kept constant despite varying trajectory or stiffness of walls. However, since the obstacles are frequently encountered during cleaning or climbing, the diatomite rags should change its moving direction or the ROPE RIDE should lift up the rags to avoid the obstacles. Therefore, the cleaning unit must be properly controlled during both cleaning and climbing of ROPE RIDE. Since existing approaches cannot resolve these difficulties, a new position-based impedance control scheme is proposed in this paper, which enables the ROPE RIDE to keep the contact force constant against external disturbances such as varying trajectories and stiffness.

3. Position-based Impedance Control for Force Tracking

3.1 Proposed impedance control

The impedance model for the proposed position-based impedance control scheme is written as follows:

$$M\ddot{x}_{dc}+B\dot{x}_{dc}+Kx_{dc}=F \tag{1}$$

where M, B and K are the target mass, damping and stiffness parameters for the impedance control. x_{dc} denotes the trajectory correction defined by the difference between desired and compliant trajectories x_d and x_c of manipulator. Note that the compliant trajectory is used to reflect that the trajectory of environment may change even slightly due to its shape or stiffness. F corresponds to the real contact force.

The proposed position-based impedance control scheme is given by

$$\begin{cases} K(t)=\left(k_pE_f+k_d\dot{E}_f+k_i\int_0^t E_f(\tau)d\tau\right)x_{dc}^{-1}+k_0 \\ x_d=x_d^0-\eta x_{dc} \end{cases} \tag{2}$$

where k_0 and x_d^0 denote the modified target stiffness and the initial condition for the desired trajectory, respectively. E_f is the force tracking error defined by the difference between the real contact and reference forces $E_f=F_{ref}-F$, and k_p, k_d and k_i are the proportional, derivative and integral control gains, respectively. η is the positive control gain for the desired trajectory correction.

It is worthwhile to note that the proposed impedance control scheme consists of stiffness adaptation as well as reference position correction, where the target stiffness is adapted by a PID control using the force tracking error while the reference position is adjusted to improve the force tracking capability effectively. In combination with the stiffness adaptation in Eq. (2), Eq. (1) becomes

$$M\ddot{x}_{dc}+B\dot{x}_{dc}+k_0x_{dc}=F_{ref}-(1+k_p)E_f-k_d\dot{E}_f-k_i\int_0^t E_f(\tau)d\tau \tag{3}$$

Since $x_{dc}=x_d-x_c=x_d^0-\eta x_{dc}-x_c$ and the initial reference position x_d^0 is constant, the first and second derivatives of the trajectory correction are given by

$$\dot{x}_{dc}=\frac{\dot{x}_c}{1+\eta} \quad \text{and} \quad \ddot{x}_{dc}=-\frac{\ddot{x}_c}{1+\eta} \tag{4}$$

Substituting Eq. (4) into Eq. (3) yields

$$\begin{aligned} &M\ddot{x}_c+B\dot{x}_c+k_0x_c-k_0x_d^0+(1+\eta)F_{ref} \\ &=(1+\eta)\left\{(1+k_p)E_f+k_d\dot{E}_f+k_i\int_0^t E_f(\tau)d\tau\right\} \end{aligned} \tag{5}$$

Without loss of generality, it is assumed that the contact force F can be expressed by $F=k_e(x-x_e)$ where x and x_e are the trajectories of the manipulator and the environment, respectively. k_e is the unknown stiffness of environment. Also, a position tracking error may occur in spite of efforts of the inner-loop position controller for the motor drive, that is, $x_e=x+\delta x$ where δx denotes the position tracking error of inner-loop controller. As a result, the force tracking error is written by

$$E_f=F_{ref}-F=F_{ref}-k_e(x-x_e) \tag{6}$$

Eq. (6) implies that the real trajectory of the manipulator can be approximated by

$$x=x_e+\frac{F_{ref}-E_f}{k_e} \tag{7}$$

It is worthwhile to note that the trajectory x_e and stiffness k_e of environment are unknown and also, x_e can be changed so that $\ddot{x}_e\neq 0$ and $\dot{x}_e\neq 0$. Under the assumption that the stiffness of environment is constant, the following derivatives can be obtained from Eq. (7):

$$\dot{x}=\dot{x}_e+\frac{\dot{F}_{ref}-\dot{E}_f}{k_e} \quad \text{and} \quad \ddot{x}=\ddot{x}_e+\frac{\ddot{F}_{ref}-\ddot{E}_f}{k_e} \tag{8}$$

Substituting Eq. (8) into Eq. (5) gives

$$\begin{aligned} &M\left(\ddot{x}_e+\frac{\ddot{F}_{ref}-\ddot{E}_f}{k_e}+\delta\ddot{x}\right)+B\left(\dot{x}_e+\frac{\dot{F}_{ref}-\dot{E}_f}{k_e}+\delta\dot{x}\right) \\ &+k_0\left(x_e+\frac{F_{ref}-E_f}{k_e}+\delta x\right)=(1+\eta)\{(1+k_p)E_f+k_d\dot{E}_f \\ &+k_i\int_0^t E_f(\tau)d\tau\Big\}+k_0x_d^0-(1+\eta)F_{ref} \end{aligned} \tag{9}$$

Supposing that the first and second derivatives of position error of inner-loop controller are relatively smaller than those of the trajectory of environment, let's define a new variable $\overline{x_e}$ by $\overline{x_e}=x_e+\delta x$ which enables to deal with both varying trajectory of environment and undesired position tracking error simultaneously. Using this definition, Eq. (9) becomes

$$\begin{aligned} &M\ddot{\overline{x}}_e+B\dot{\overline{x}}_e+k_0\overline{x}_e+\frac{1}{k_2}[M\ddot{F}_{ref}+B\dot{F}_{ref}+(k_0+k_e(1+\eta))F_{ref}] \\ &=\frac{1}{k_2}(M\ddot{E}_f+B\dot{E}_f+k_0E_f)+(1+\eta)\{(1+k_p)E_f+k_d\dot{E}_f \\ &+k_i\int_0^t E_f(\tau)d\tau\Big\}+k_0x_d^0 \end{aligned} \tag{10}$$

Define the Laplace transforms of the trajectory of environment combined with the position error, the force tracking error, the initial reference trajectory and the reference force as $L\{\overline{x_e}\}=X_e(s)$, $L\{E_f\}=E_f(s)$, $L\{x_d^0\}=X_d^c(s)$ and $L\{F_{ref}\}=F_{ref}(s)$, respectively. Then, in the Laplace domain, Eq. (10) can be rewritten by

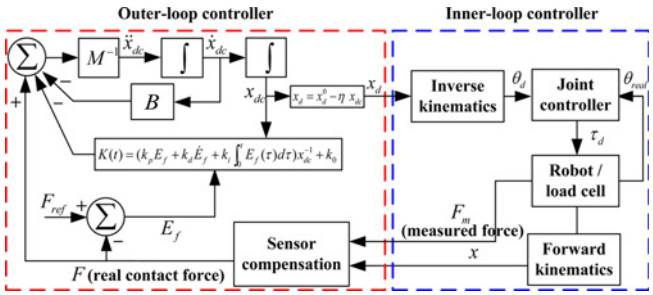

Fig. 3 Block diagram of proposed position-based impedance control scheme for force tracking of manipulator

$$(Ms^2+Bs+k_0)X_e(s)+\frac{1}{k_e}[Ms^2+Bs+k_0(k_0+k_e(1+\eta))]F_{ref}(s)$$
$$=\frac{1}{k_e}(Ms^2+Bs+k_0)E_f(s)+k_0X_d^0(s)+(1+\eta)\left(1+k_p+k_ds+\frac{k_i}{s}\right)E_f(s) \quad (11)$$

After rearranging each term in Eq. (11), the following relation between the force tracking error, varying trajectory of environment and the reference force can be obtained as follows:

$$E_f(s)=\frac{k_es(Ms^2+Bs+k_0)}{\Lambda(s)}X_e(s)$$
$$+\frac{s[Ms^2+Bs+(k_0+k_e(1+\eta))]}{\Lambda(s)}F_{ref}(s)-\frac{k_0k_es}{\Lambda(s)}X_d^0(s) \quad (12)$$

where $\Lambda(s)$ corresponds to the characteristic equation of transfer function from the trajectory of environment (or the reference force) to the force tracking error given by $\Lambda(s)=Ms^3+a_0s^2+a_1s+a_2$. M is set to be 1 and $a_0=B+k_e(1+\eta)k_d$, $a_1=k_0+k_e(1+k_p)(1+\eta)$ and $a_2=k_e(1+\eta)k_i$. In fact, $X_d^0(s)=x_d^0/s$ holds since the initial reference trajectory x_d^0 is assumed to be constant.

The block diagram of proposed position-based impedance control scheme for force tracking of manipulator is described in Fig. 3, where the real contact force is obtained by calibrating the force measured by using the load cell. It is worthwhile to note that in the proposed impedance control scheme, the reference trajectory and the target stiffness are simultaneously updated because these two terms mainly contribute the force tracking error of classic impedance control in the steady state.

3.2 Stability and performance analysis

In order to derive the stability condition for the proposed position-based impedance control scheme, the Routh-Hurwitz array for Eq. (12) is constructed as follows:

s^3	1	a_1
s^2	a_0	a_2
s^2	$(a_0a_1-a_2)/a_0$	0
s^0	a_2	0

From the Routh-Hurwitz array, $a_0>0$, $a_2>0$, $(a_0a_1-a_2)/a_0>0$ should be satisfied to guarantee the stability of proposed impedance control scheme. It should be noted that the proportional, derivative and integral control gains k_p, k_d and k_i as well as the trajectory modification gain η are all positive so that $a_i>0$, i=0, 1 and 2 are naturally ensured and $a_0a_1-a_2>0$ will guarantee the stability of proposed impedance control law. Recall that the last condition can be rewritten as follows:

$$a_0a_1-a_2=(B+k_e(1+\eta)k_d)\times(k_0+k_e(1+k_p)(1+\eta))-k_e(1+\eta)k_i$$
$$>k_e(1+\eta)k_d\times k_e(1+k_p)(1+\eta)-k_e(1+\eta)k_i$$
$$=k_e^2(1+\eta)^2\left((1+k_p)k_d-\frac{k_i}{k_e(1+\eta)}\right)>0$$

From the above inequality, $a_0a_1-a_2>0$ can be guaranteed if

$$(1+k_p)k_d-\frac{k_i}{k_e(1+\eta)}>0 \quad (13)$$

It is worthwhile to note that k_e can be assumed sufficiently large so that it is easy to choose control gain parameters k_p, k_d, k_i and η to satisfy Eq. (13).

Now, suppose that the trajectory of environment changes as if it is a unit step, that is, $X_e(s)=1/s$. For the constant reference force F_{ref} whose Laplace transform is given by $F_{ref}(s)=F_{ref}/s$, the force tracking error E_f in the steady state can be obtained by using the Final Value Theorem as follows:

$$\lim_{t\to\infty}E_f=\lim_{s\to0}sE_f(s)=\lim_{s\to0}s\left\{\frac{k_es(Ms^2+Bs+k_0)}{\Lambda(s)}\frac{1}{s}\right.$$
$$\left.+\frac{s[Ms^2+Bs+(k_0+k_e(1+\eta))]}{\Lambda(s)}\frac{F_{ref}}{s}-\frac{k_0k_es}{\Lambda(s)}\frac{x_d^0}{s}\right\}=0 \quad (14)$$

which proves that the proposed impedance control scheme enables the manipulator to track the reference force in the steady state in spite of sudden change in the trajectory of environment. Recall that in fact, the reference force in Eq. (14) is equal to a step function, which also implies that the proposed impedance control scheme ensures the zero force tracking error in the steady state even though the reference force changes suddenly.

Compared to existing impedance control methods, the proposed position-based impedance control scheme ensures the zero force tracking performance in the steady state against drastic changes in the trajectory of environment and the reference force without detailed information on the dynamics of robot manipulator. In addition, the control parameters are easily chosen and tuned to satisfy the stability condition for the proposed impedance control scheme.

4. Experiments and Discussions

In this section, the force tracking capability of proposed position-based impedance control scheme is investigated through the extensive experiments using the wall-cleaning unit in comparison with that of the PID type generalized impedance control algorithm against various types of walls. Note that the PID type generalized impedance control algorithm combines the trajectory correction with the force tracking error in the following manner:

$$M\ddot{x}_{dc}+B\dot{x}_{dc}+Kx_{dc}=-k'_pE_f-k'_d\dot{E}_f-k'_i\int_0^t E_f(\tau)d\tau \quad (15)$$

where k'_p, k'_d and k'_i correspond to the proportional, derivative and integral control gains, respectively. Recall that the zero force tracking error in Eq. (15) implies the zero trajectory correction so that the

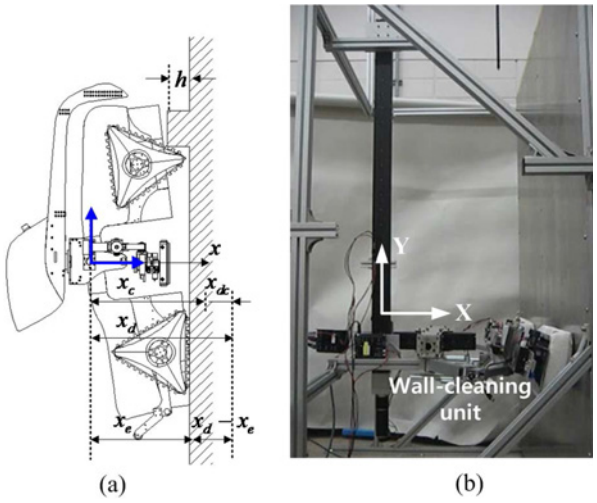

Fig. 4 (a) Schematic diagram of ROPE RIDE equipped with wall-cleaning unit and (b) set-up for force tracking experiments

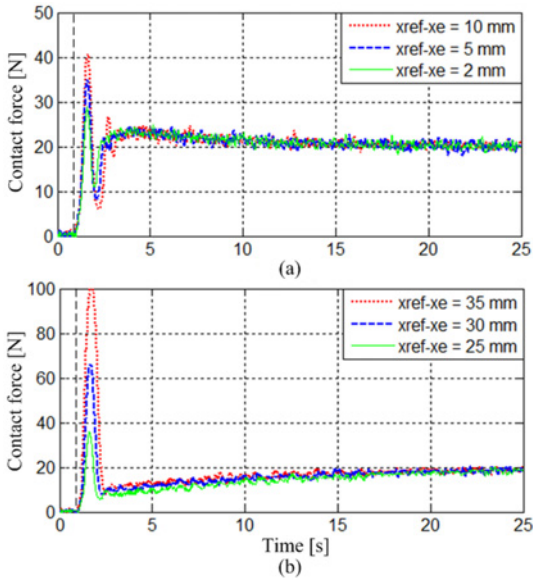

Fig. 5 Contact force responses of (a) proposed and (b) typical PID type impedance controls for different trajectories of wall

compliant trajectory of manipulator is exactly same as the desired one, which may be possible if there is no constraint on the trajectory of manipulator. However, it is quite difficult to make the compliant trajectory equal to the desired one because the real trajectory of manipulator is highly restricted by a wall of building so that the PID type impedance control in Eq. (15) cannot achieve both zero force tracking error and zero trajectory correction simultaneously.

Fig. 4 shows the schematic diagram of ROPE RIDE equipped with the wall-cleaning unit and the photo of force tracking experimental setup. The desired trajectory of manipulator and the trajectory environment are denoted by x_d and x_e in Fig. 4(a), which are the distances from the R-joint of ROPE RIDE to the end of cleaning unit and the wall, respectively. As shown in Fig. 4(b), the 2-DOF test bench using the wall-cleaning unit is designed to imitate the motion of ROPE RIDE climbing up or overcoming an obstacle. Therefore, the cleaning unit can move parallel to the wall (along the Y-axis) and also, push the rags toward the wall (along the X-axis) during wall-cleaning.

Recall that in the previous research, the periodical oscillations are observed while moving two diatomite rags from side to side, which is because the bar of wall-cleaning unit supporting two rags is not sufficiently rigid.[15] As a result, undesired bending of bar of wall-cleaning unit happens to cause the stiffness of wall k_e to change periodically, that is, k_e becomes maximal (or minimal) when two rags are very close (or far away). Since this oscillation can be solved by increasing the stiffness of wall-cleaning unit or decreasing the desired contact force, the objective of experiments in this study is focused on verifying the force tracking performance of proposed position-based impedance control scheme without moving two rags.

The implementation of proposed impedance control algorithm as well as data acquisition is carried out by using the NI compact RIO with the help of LabVIEW. During all experiments, the data is acquired with the sampling time of 160 Hz. The parameters of target impedance model are selected as $(M, B, k_0) = (1, 176, 58000)$, which drives the behavior of the manipulator similar to that of the second order system with the resonant frequency of 240 rad/s and the damping coefficient of 0.37. Also, the proportional, derivative and integral control gains are chosen as $(k_p, k_d, k_i) = (30, 4, 5)$ and the trajectory correction gain η is set to be 0.02, respectively. Note that these control gains are chosen to satisfy the stability condition in Eq. (13).

First, the force tracking capability of proposed impedance control scheme is investigated with different trajectories of wall so that the distances between the wall and the manipulator $x_d - x_e$ are chosen to be 2 mm, 5 mm and 10 mm, respectively and the desired contact force is set to be 20 N. Figs. 5(a) and 5(b) show the contact force responses of proposed impedance control scheme and PID type generalized impedance control, respectively. The dotted black lines in Figs. 5(a) and 5(b) indicate the moment when the end of wall-cleaning unit begins to contact with the wall. Since the end of wall-cleaning unit did not come into contact with the wall even with the distance of 10 mm when applying the PID type generalized impedance control, the distance $x_d - x_e$ is adjusted to be 25 mm, 30 mm and 35 mm, respectively. Therefore, as shown in Fig. 5(b), the initial contact force obtained by the PID type generalized impedance control becomes larger than that obtained by the proposed impedance control. It is worthwhile to note that the initial contact force plays important role in determining the stability of wall-climbing mobile platform in that a larger initial contact force will prevent the wall-climbing mobile platform from stably climbing the wall.

Compared to the PID type generalized impedance control, the proposed impedance control scheme ensures better force tracking performance as well as shorter settling time. In Fact, recalling that the Y-axis scaling of Fig. 5(b) is larger than that of Fig. 5(a), the contact force obtained by the proposed impedance control scheme converges to the desired one within a bound of less than 2.5 N in about 10 sec while that obtained by the PID type generalized impedance control still is far away from the desired one. It is noted that the control gains like k_p, k_d, k_i and η adopted for the experiments in this study are not optimally chosen. Therefore, these gains may be optimized to improve the

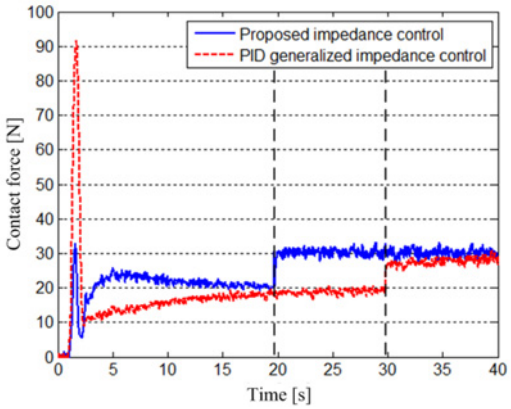

Fig. 6 Contact force responses of proposed and typical PID type impedance controls for varying desired forces

performance of proposed impedance control scheme.[16]

Another experiment is carried out by using the same control gains with a varying desired force. Although the stiffness of environment is assumed to be constant in Section 2, it may change if the materials of environment are different, which will lead to unexpected change of the contact force. The experimental results are shown in Fig. 6, where the dotted black lines indicate the moment when the desired force is increased from 20 N to 30 N. Recall that for the proposed and PID type generalized impedance control methods, the distances $x_d - x_e$ are set to be 5 mm and 35 mm, respectively so that the initial contact force of PID type generalized impedance control method is much larger than that of proposed impedance control. When the desired force is suddenly changed, the contact force of PID type generalized impedance control is not sufficiently increased as shown in Fig. 6. Therefore, while the contact force of proposed impedance control scheme can track the desired one without delay despite change of desired contact force, the contact force of PID type generalized impedance control method still suffers from slow and insufficient response.

The other experiment is performed under the assumption that the wall-cleaning unit overcomes the obstacle whose height h in Fig. 4(a) is given by 20 mm. Figs. 7(a) and 7(b) show the experimental results obtained by the proposed and PID type generalized impedance control methods, respectively. The left dotted lines in Figs. 7(a) and 7(b) indicate the moment when the wall-cleaning unit is lifted up from the wall to avoid the obstacle so that the resulting contact forces are decreased. The right dotted lines in Figs. 7(a) and 7(b) indicate the moment when the wall-cleaning unit is lifted down to contact with the wall so that the resulting contact forces are increased. Note that since the rising/settling times of PID type generalized impedance control are much longer, the time duration of experiment using the PID type generalized impedance control is chosen to be much longer than that of proposed impedance control scheme. As confirmed in Figs. 7(a) and 7(b), the contact force obtained by the proposed impedance control scheme converges to the desired one more quickly compared to the PID type generalized impedance control.

Note that the contact force contains certain noise components as shown in Figs. 5, 6 and 7, whose magnitude in the steady state is limited within a bound of 2.5 N. In fact, since a rubber is installed

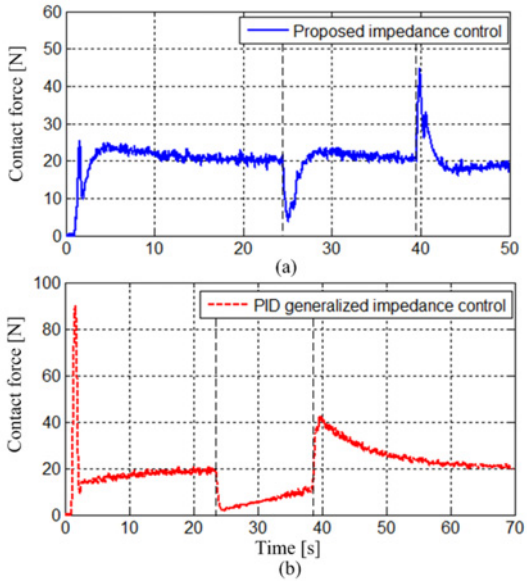

Fig. 7 Contact force responses of (a) proposed and (b) typical PID type impedance controls for varying trajectories of wall

between the rags and the center bar of wall-cleaning unit in order to increase the flexibility of wall-cleaning unit over various trajectories of wall, unexpected force stemming from small swing of rags may be continuously measured by the load-cell when the rag of wall-cleaning unit keeps in a surface-contact with the wall. The resulting contact force may suffer from much noise compared to the case of point-contact, which must be resolved in the future research.

It is worthwhile to note that the stability of PID type generalized control method in Eq. (15) can be ensured if $Bk_p - Mk_i > 0$ holds, which does not include the stiffness of environment so that choice of control gains may be less constrained in comparison with the proposed impedance control scheme in Eq. (13). However, the PID type generalized impedance control method does not seem to be suitable for force tracking tasks whose trajectory is highly restricted because the PID type generalized impedance control method cannot achieve both force tracking and position tracking. Therefore, the dynamic response of PID type generalized control method is quite slow and insufficient although its initial contact force is much larger than that of proposed impedance control scheme.

5. Conclusions

In this paper, the position-based impedance control scheme is proposed for force tracking of wall-cleaning unit installed in the wall-climbing mobile platform ROPE RIDE. Compared to existing impedance control methods, the proposed impedance control scheme ensures zero force tracking error in the steady state under varying trajectory and unknown stiffness of environment without dynamic models and uncertainties of wall-cleaning unit. The stability condition required for the proposed impedance control scheme is derived by using the Routh-Hurwitz array, which is used to choose the control gains. Since the choice of control gains to satisfy the stability condition

is quite simple, the optimization method can be applied to improve the force tracking capability of proposed impedance control scheme. The force tracking capability of proposed impedance control scheme is verified through the experimental comparison with the PID type generalized impedance control method, which implies that against varying trajectory and stiffness of wall, the proposed scheme enables the wall-cleaning unit to track the desired force with a bound of 2.5 N in the steady state.

ACKNOWLEDGEMENT

This research was supported in part by Basic Science Research Program through the National Research Foundation of Korea (NRF) grant funded by the Ministry of Science, ICT & Future Planning (No 2012R1A1A1010046) and in part by the Ministry of Education (No 2014R1A1A2055668).

REFERENCES

1. Raibert, M. H. and Craig, J. J., "Hybrid Position/Force Control of Manipulators," Journal of Dynamic Systems, Measurement, and Control, Vol. 103, No. 2, pp. 126-133, 1981.
2. Khatib, O., "A Unified Approach for Motion and Force Control of Robot Manipulators: The Operational Space Formulation," IEEE Journal of Robotics and Automation, Vol. 3, No. 1, pp. 43-53, 1987.
3. Hogan, N., "Impedance Control: An Approach to Manipulation," Proc. of American Control Conference, pp. 304-313, 1984.
4. Kumar, N., Panwar, V., Sukavanam, N., Sharma, S. P., and Borm, J.-H., "Neural Network based Hybrid Force/Position Control for Robot Manipulators," Int. J. Precis. Eng. Manuf., Vol. 12, No. 3, pp. 419-426, 2011.
5. Kang, S., Komoriya, K., Yokoi, K., Koutoku, T., Kim, B., and Park, S., "Control of Impulsive Contact Force between Mobile Manipulator and Environment using Effective Mass and Damping Controls," Int. J. Precis. Eng. Manuf., Vol. 11, No. 5, pp. 697-704, 2010.
6. Kim, Y.-L., Song, H.-C., and Song, J.-B., "Hole Detection Algorithm for Chamferless Square Peg-in-Hole based on Shape Recognition using F/T Sensor," Int. J. Precis. Eng. Manuf., Vol. 15, No. 3, pp. 425-432, 2014.
7. Kim, J.-Y., Yang, U.-J., and Park, K., "Design, Motion Planning and Control of Frozen Shoulder Rehabilitation Robot," Int. J. Precis. Eng. Manuf., Vol. 15, No. 9, pp. 1875-1881, 2014.
8. Kim, C. Y., Lee, M. C., Wicker, R. B., and Yoon, S.-M., "Dynamic Modeling of Coupled Tendon-Driven System for Surgical Robot Instrument," Int. J. Precis. Eng. Manuf., Vol. 15, No. 10, pp. 2077-2084, 2014.
9. Seraji, H. and Colbaugh, R., "Force Tracking in Impedance Control," The International Journal of Robotics Research, Vol. 16, No. 1, pp. 97-117, 1997.
10. Cho, H. C., Park, J. H., Kim, K., and Park, J.-O., "Sliding-Mode-based Impedance Controller for Bilateral Teleoperation Under Varying Time-Delay," Proc. of IEEE International Conference on Robotics and Automation, Vol. 1, pp. 1025-1030, 2001.
11. Iwasaki, M., Tsujiuchi, N., and Koizumi, T., "Adaptive Force Control for Unknown Environment using Sliding Mode Controller with Variable Hyperplane," JSME International Journal Series C Mechanical Systems, Machine Elements and Manufacturing, Vol. 46, No. 3, pp. 967-972, 2003.
12. Jung, S., Hsia, T. C., and Bonitz, R .G., "Force Tracking Impedance Control of Robot Manipulators under Unknown Environment," IEEE Transactions on Control Systems Technology, Vol. 12, No. 3, pp. 474-483, 2004.
13. Lee, K., and Buss, M., "Force Tracking Impedance Control with Variable Target Stiffness," Proc. of the 17th IFAC World Congress, pp. 6751-6756, 2008.
14. Seo, K., Cho, S., Kim, T., Kim, H. S., and Kim, J., "Design and Stability Analysis of a Novel Wall-Climbing Robotic Platform (Rope Ride)," Mechanism and Machine Theory, Vol. 70, pp. 189-208, 2013.
15. Kim, T., Seo, K., Kim, J.-H., and Kim, H. S., "Adaptive Impedance Control of a Cleaning Unit for a Novel Wall-Climbing Mobile Robotic Platform (Rope Ride)," Proc. of IEEE/ASME International Conference on Advanced Intelligent Mechatronics (AIM), pp. 994-999, 2014.
16. Lee, K. and Kim, J., "Controller Gain Tuning of a Simultaneous Multi-Axis Pid Control System using the Taguchi Method," Control Engineering Practice, Vol. 8, No. 8, pp. 949-958, 2000.